Nigerian Journal of Technology (NIJOTECH)
Vol. 44, No. 2, June, 2025, pp.252 - 261
www.nijotech.com

Print ISSN: 0331-8443
Electronic ISSN: 2467-8821
https://doi.org/10.4314/njt.v44i2.9

CFD MODELLING OF THE EFFECT OF MECHANICAL VENTILATION ON HYDROGEN LEAK AND DISPERSION IN A PARTIALLY ENCLOSED SPACE

AUTHORS:
M. S. Lawal[1], U. M. Abdullahi[2], A. M. Na'ina[3], A. Adeleke[4], S. Jesuloluwa[5,*] and R. E. Abuh[6]

AFFILIATIONS:
[1,2,3]Aerospace Engineering Department, Air Force Institute of Technology, Kaduna, Nigeria.
[4,5]Mechanical Engineering Department, Nile University of Nigeria, Abuja, FCT, Nigeria.
[6]Mechanical Engineering Department, Federal University of Technology Minna, Niger State, Nigeria.

***CORRESPONDING AUTHOR:**
Email: seun.jesuloluwa@nileuniversity.edu.ng

ARTICLE HISTORY:
Received: 28 October, 2024.
Revised: 14 May, 2025.
Accepted: 18 May, 2025.
Published: 07 July, 2025.

KEYWORDS:
CFD simulation, Hydrogen dispersion, Hydrogen leakage, Fire risk, Mechanical ventilation, Hydrogen gas, Test cell.

ARTICLE INCLUDES:
Peer review

DATA AVAILABILITY:
On request from author(s)

EDITORS:
Ozoemena Anthony Ani

FUNDING:
None

Abstract

This study employed a Computational Fluid Dynamics (CFD) approach based on STAR-CD code to investigate the effect of mechanical ventilation on hydrogen gas leaks and diffusion in partially enclosed space. It is a case study of a homogenous charged compression ignition engine (HCCI) laboratory of the Mechanical Engineering Department, University College London (UCL). The 3-D modelling was based on the geometry as well as airflow designed for the test laboratory. Two turbulence models and three differencing schemes were employed on two grid refinement levels. All the differencing Schemes predicted a similar velocity profile and hydrogen concentration below 25% of the lower flammability limit (LFL) in most parts of the test laboratory. Although the predicted hydrogen mass fraction from the steady state simulation does not resolve the buoyant shape of the gas, the time-dependent solution captures the buoyant characteristic of hydrogen. It revealed that the hydrogen gas initially rises to a height 0.55cm above the exit towards the ceiling, from where it gradually diffuses in a radial pattern to a homogenous non-flammable concentration in the room. This predicted pattern of hydrogen gas dispersion is consistent with experimental data. Therefore, a small hydrogen leak of the type and at the airflow rates investigated in this study does not pose a risk of fire in most parts of the Engine Test laboratory; except in the region very close to the leak source.

1.0 INTRODUCTION

The use of hydrogen fuel to complement petroleum and natural gas as an energy source is widely accepted as cost-effective and more sustainable. Hence, hydrogen is deemed to be the ideal fuel for the future and is considered suitable for use not only in fuel cells but also in internal combustion engines. Being the lightest element, hydrogen has a high energy capacity per unit mass, releasing three times more energy than gasoline with less emission of pollutants [1], [2], [3]. Due to these benefits, there is a tendency for a global increase in utilization of hydrogen in the transportation sector. The light weight of hydrogen, however, gives it a strong diffusion coefficient of 0.76 cm^2/s in excess air at atmospheric pressure and room temperature [4]. This makes hydrogen highly susceptible to leakage through small holes and cracks, forming a flammable mixture with air. Hydrogen being an odorless and colourless gas makes it difficult to detect its leakage by humans, which increases the risk of fire accidents.

HOW TO CITE:
Lawal, M. S., Abdullahi, U. M., Na'ina, A. M., Adeleke, A., Jesuloluwa, S., and Abuh, R. E. "CFD Modelling Of The Effect Of Mechanical Ventilation On Hydrogen Leak And Dispersion In A Partially Enclosed Space", *Nigerian Journal of Technology*, 2025; 44(2), pp. 252 – 261; https://doi.org/10.4314/njt.v44i2.9

In the case of hydrogen leak in open air, the natural buoyancy of the gas facilitates fast dilution and dispersal away from the leak source. However, for hydrogen leak in an enclosure, the natural buoyancy is lost [5]. Hence, leaking hydrogen gas can be trapped, forming a flammable mixture with air. Therefore, insufficient ventilation causes a high risk of fire and explosion from the accidental release of hydrogen. The relative ease of leak, diffusion, and accumulation of hydrogen gas in an enclosed and semi-enclosed space, and the associated fire hazard in the presence of an ignition source, explains why leakage of the gas is considered unsafe. As such, safe and effective utilization of hydrogen requires understanding how the gas disperses in an enclosure with mechanical ventilation, which is essential for safety risk assessment.

Different approaches have been employed to determine the effectiveness of ventilation due to hydrogen leakage and dispersion in an enclosure. Tanaka et al [6] carried out an experimental study of hydrogen leakage, dispersion and explosion in a storage room 4 x 6 x 5m^3. The hydrogen was released through one of two nozzles of diameter 8mm and 1.6 mm. The room was equipped with natural ventilation openings located along the top 1m of either two or all four sidewalls. Results from the dispersion experiments revealed that leak diameter, volume of hydrogen released and ventilation characteristics of the room significantly affect the hydrogen concentration. The study concluded that designing a room to have sufficient ventilation is effective in reducing the concentration of hydrogen, such that there was only a small hazardous area around the release nozzle [6]. Brzezinska [2], [3] conducted an experimental and CFD study of mechanical ventilation effects on hydrogen dispersion in an enclosure under different release conditions. The experiments were performed for hydrogen leak of 1.63 x 10^{-3} m^3/s through single and multi-point nozzles. It was found that there was significantly higher hydrogen stratification and buoyancy in single-point nozzle release because the Froud number was five orders of magnitude higher than that of multi-point nozzle. The study concluded that the lower the Froud Number, the lower the buoyancy force influences hydrogen dispersion.

The approach of CFD simulation in predicting hydrogen dispersion has the added advantage of being safer and cost-effective, as well as being able to provide more detailed data on hydrogen concentration, flammable region and spatial distribution [6]. Consequently, the technique of CFD has been employed to study hydrogen dispersion in exit vent mast [1], double ferrule joints [7], partially confined spaces [8] underground parking lots [9], [10],[11] as well as residential area and fuel cell vessel room [10]. Prasad et al., [15] conducted a CFD analysis on the effect of wind and buoyancy on hydrogen release and dispersion in a compartment with vents at multiple levels. The study highlighted that in the case where the air inlet is at a low level (near the floor of the enclosure) and the air exit is at a high-level (near the ceiling), wind adds to the buoyancy-driven flow. On the other hand, if the air inlet is at the upper vent and the air exit is at the lower vent, then the wind opposes the buoyancy-driven flow. In the latter scenario, the natural buoyancy of the gas can be reduced and its flow direction could change, depending on the strength of the wind.

The study of Blaylock and KlebanoffI [1] investigated the dispersion pattern of hydrogen release from a vent mast of a fuel cell vessel. CFD tool was used to model the gas released from 250-bar hydrogen storage tanks through the vent mast, with a crosswind blowing horizontally at 5 mph (2.24m/s). It was shown that the effect of the wind on hydrogen gas dispersion strongly depends on the gas exit velocity. For high release velocity, (800 -900 m/s), the hydrogen flow is strongly momentum-driven, with modest cross-wind influence. In the case of low hydrogen exit velocity (20-10m/s), the hydrogen gas is readily entrained in the wind flow and blown sideways. The additional calculation was performed with the hydrogen exiting at 8.6m/s, under a downward crosswind blowing at 45^o angle. The results show that, despite the inherent buoyancy of hydrogen gas, the wind blows the gas downward [1]. The study of Lawal et al. [13] reported similar findings in the prediction of wake-stabilised jet flames in a cross-wind flow using the Reynolds Average Nervier Stokes (RANS) framework.

A CFD benchmark study of hydrogen release and dispersion in a confined space with natural ventilation using helium as a surrogate gas was reported by Seike et al. [14]. The three test cases investigated involved releasing helium from varying orifice sizes at the centre of the enclosure. The study employed three CFD codes, ANSYS Fluent, ADREA-HF and ANSYS CFX and three turbulence models, transitional SST, standard $k-\varepsilon$ and Smagorinski Large Eddies Simulation (LES). The study reported good agreement between the predicted and experimentally measured helium concentrations. In the case of the release vent with the smallest vertical extension, all the CFD codes over-predicted the concentration in the lower part of the enclosure at a steady state.

Based on the review of related literature, it is observed, that in most of the CFD studies that employed actual hydrogen gas for modeling, the geometry often employed were those of residential or private garages and parking lots. These are not the same with the configuration of the enclosure in the Engine Test laboratory (Test Cell 4) under investigation in this study. Since extrapolating results from one geometry to another is not reliable, it is expedient to carry out detailed modelling of hydrogen leak and dispersion based on the actual geometry of the Engine Test Cell 4 under investigation. It is a case study of the highly charged compression ignition (HCCI) engine laboratory at the Mechanical Engineering Department, University College, London (UCL). The Laboratory was modified to adapt a car diesel engine to an HCCI engine using hydrogen fuel. This necessitates an in-depth investigation of how hydrogen leak in the laboratory behaves. Therefore, this study seeks to determine the influence of the mechanical ventilation designed for the laboratory on hydrogen gas dispersion, which enables an understanding of the nature of the risk of inadvertent release of hydrogen gas in the Test Cell.

2.0 EXPERIMENTAL FACILITY

2.1 Geometry and Airflow Through the Engine Test Laboratory

The dimension of the HCCI engine laboratory at UCL is 4.55m x 3.71m x 3.45m (height), translating to 58.23m^3 volume, as shown in Figure 1. It is a partially enclosed room with air vents provided for forced ventilation. The inlet vent is a rectangular slot of dimension 1.1m x 0.55m, located 17.5cm below the ceiling inclined at 45^o to the horizontal. The outlet vents comprise two openings on the floor of the test room of dimensions 2.55m x 0.23m. Two variable speed fans working in parallel facilitate forced air extraction through the air exit vents, each at maximum and minimum volume flow rates of 0.635m^3/s and 0.317m^3/s, respectively [Nylander L, UCL facility and estate department]. The area A_f of each exit vent is 0.5865m^2, and the volume flow rate at low exit velocity of 0.567m/s is 0.634m^3/s. Thus, the air change per hour (ACH) is estimated to be about 40ACH. The experimental facilities included in the CFD modeling are shown in Figure 2(a). The engine test bed is raised 2m above the floor. Hydrogen gas used by the test engine is delivered at 4bar and 15^{o}C through the 0.0254m diameter stainless steel pipe.

2.2 Simplified Model of the Test Cell Laboratory

In the simplified model of the Test Cell, the test engine, dynamometer and test bed geometry were modelled as rectangular blocks, see Figure 2 (a). Also, the leak source was assumed to be on the engine test bed. The area of the pipe was outlined as a circular section on the engine block of the same diameter as the pipe (0.0254m). The hydrogen gas with a density 0.33 kg/m^3 leaks through a 0.0254m diameter orifice at a velocity 20.86m/s (mass flow rate is $3.49 * 10^{-4}\ kg/s$). Thus, hydrogen is assumed to leak through an area marked red in Figure 2(b), representing 10% of the pipe diameter. These assumptions are used for the simulation of the hydrogen leakage.

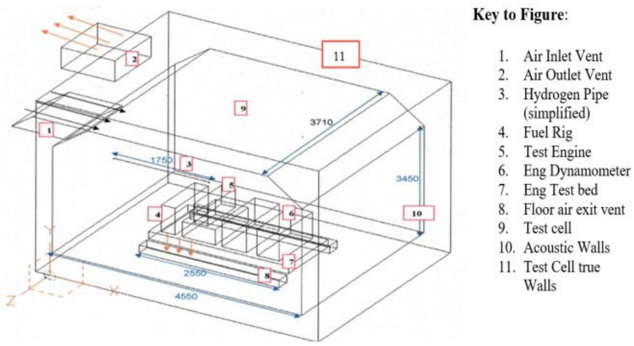

Figure 1: Schematic of the engine test cell and experimental facilities

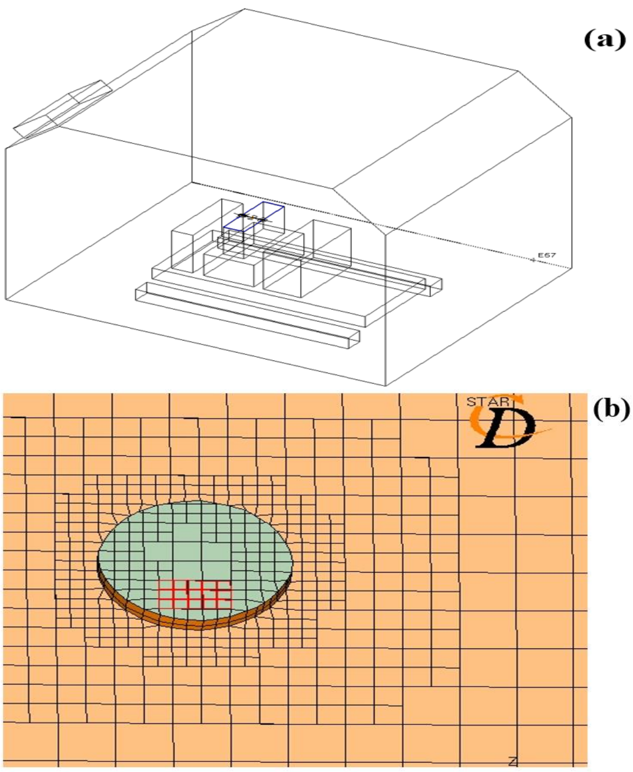

Figure 2: **(a)** 3D schematic of the simplified model showing pipe region, **(b)** Leak area is defined on 15 faces on pipe

The Reynolds number R_e of the airflow through the Test cell can be calculated based on:

$$Re = \frac{VD_h\rho}{\mu} = \frac{VD_h}{\nu} \quad [15] \qquad (1)$$

Where, v is the average velocity of the airflow, $D_h = \frac{2ab}{a+b}$ is the equivalent hydraulic diameter of the air exit, a and b are the lengths of the sides of the test cell, μ is the dynamic viscosity of air, and $\nu$is the kinematic viscosity of air.

Thus, the Reynolds number of the flow through each air exit vent is computed as $6.87 * 10^4$, which yields an incompressible turbulent flow. Based on the design of the Test Cell, make-up air is drawn through the air inlet vent below the ceiling by the pressure drop created due to air extraction vide the floor exit vents. This implies, the exact condition of the air inlet vent is unknown and is calculated as part of the CFD solution process.

2.3 Surface and Volume Meshing

The 3-D geometry of the Engine Test Cell 4 was prepared in IDEAS, with the surface meshes having maximum and minimum edge lengths of 113mm and 3mm, respectively, See Figure 3(a). The volume mesh generation comprises a uniform subsurface thickness of 5mm for the whole model and maximum cell sizes of 30mm. To capture more details of the leak region, a minimum cell size of 1.5mm was used to model the leak area. The total volume cells of the initial meshed model are composed of 715,512 fluid cells.

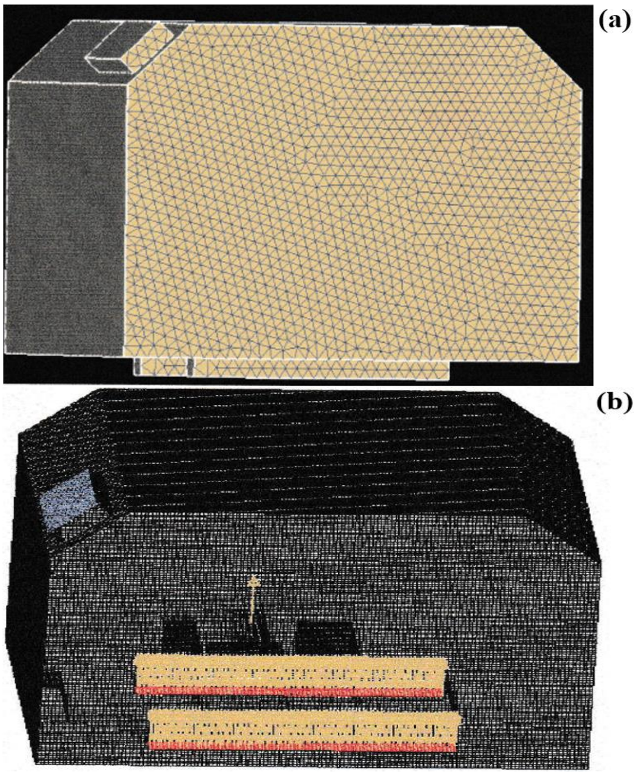

Figure 3: **(a)** Triangulated surface of the model **(b)** Final model showing volume mesh and boundary conditions

Table 1: Boundary conditions combinations

Region	Boundary Type	Velocity/Pressure	Temperature (K)	T_i	L (m)	Mass flow (m³/s)
Air Inlet Vent	Pressure	0Pa	293	0.1	0.055	-
Extraction Vent	Negative Inlet	-0.5675 m/s (Each)	293	0.1	0.127	-
Hydrogen Leak	Inlet	20.86 m/s	288	0.1	0.0004	-

2.4 Boundary Conditions

The following assumptions and simplifications were made in defining the boundary conditions appropriate to the Engine Test Cell operating conditions. For the thermo-physical setting, gravity was considered. The background fluid was air and its density variation was considered to be an ideal function of temperature. The solution was initialized at the air exit boundary for air with turbulence intensity and mixing length scale of 0.1 and 0.2275, respectively. Reference temperature and pressure were 293K and 1bar respectively. Hydrogen gas was identified as the additional scalar with its density at 15°C and 4bar evaluated as 0.33kg/m^3. Schmidt number of 0.7 was also adopted. The summary of boundary condition combinations employed is presented in Table 1 and Figure 3 (b). In the Table, T_i and L represents the turbulent intensity and length scale, respectively.

3.0 MODELING OF HYDROGEN LEAKS AND DIFFUSION

3.1 Turbulent Flow Modelling

To model the fluid flow in the Engine Test Cell, the continuity, momentum, energy and scalar transport equations were solved. To avoid the complexity of solving for instantaneous properties in turbulent flows, the Reynolds Average Nervier Stokes (RANS) form of governing equations was solved. Reynolds averaging produced unclosed terms in the RANS version of the momentum and energy equations, also known as the Reynolds stresses and Reynolds fluxes, respectively. To close and resolve the Reynolds stresses, the approach used is the standard $k - \varepsilon$ (k-epsilon) turbulence model. Solving these equations enables approximate modelling of the turbulence in flow physics.

3.2 Solution Method

The solution method was based on steady-state and transient analyses. The justification for the initial steadystate solution approach is based on the expectation that, after the initial turbulent mixing, the overall airflow and hydrogen concentration in the Test Cell will settle in a steady-like manner [5]. However, this assumption does not preclude the transient nature of the problem. SIMPLE algorithms were employed for pressure-velocity coupling and Algebraic Multi-grid (AMG) solution method was chosen. The governing equations and turbulence models were solved as implemented in the Star-CD CFD code. The Upwind Differencing Scheme (UDS) and Linear Upwind (LUD) discretization schemes were employed. The study by Venetsanos et al. [16] reported better prediction of hydrogen concentration in the jet region with the standard $k-\varepsilon$ turbulence model using Schmidt number of 0.7 combined with smaller time step and higher order convective scheme. Furthermore, the study reported both RNG and Realizable $k-\varepsilon$ turbulence models showed a tendency to overestimate hydrogen concentration in the jet region. Consequently, in this study, the Standard $k-\varepsilon$ turbulence model was employed in combination with the Upwind differencing scheme for the steady-state solution. In the time-dependent solution, the same turbulence model was used with the MARS discretization scheme.

4.0 RESULTS AND DISCUSSION

Results obtained from the simulations with coarse and refined meshes are presented in this section in terms of x-y and x-z plots in planes of the Test Cell. Therefore, the results are in the form of cross-sectional plots of velocity magnitude and hydrogen mass fraction, which highlight the key features of the airflow and hydrogen concentration in the Test Cell. In the absence of experimental data for the same laboratory flow condition investigated in this study, results obtained are compared with published solutions from closely related experiments and high-fidelity CFD simulations reported in the literature. These include the experimental and CFD results of Venetsanos et al. [16] and CFD simulation of Kuldeep et al., [12] and the experimental study of Brzezinska [2], [3]. Results for the calculated concentration of hydrogen in the Test Cell are presented in terms of mass fraction. Consequently, the lower flammability limit of hydrogen, which is 4% by volume was converted to its equivalents in mass fraction, yielding a value of 0.3% by mass.

4.1 Mesh Refinement

Grid refinement was carried out to investigate the effect of finer grids on the solution. To this end, the reference mesh of 710,000 fluid cells was uniformly refined to 1.1million cells. Meshes in the leak region were divided by a factor of 2. The results of predicted airflow distribution and hydrogen mass fraction in the test cell obtained from steady-state simulation with both the initial and refined grids are presented in Figure 4. Comparing results from the coarse and refined grid, it was found that due to grid refinement, the predicted maximum velocity in most of the domain increased by a factor of two. A possible reason for this is the decrease in numerical diffusion from the refined grid, which leads to improved capture of hydrogen concentration in the leak region. However, further refinement of the grid to 1.5 million cells did not result in significant changes in the results obtained. Consequently, subsequent calculations were done with the grid with 1.1 million fluid cells.

4.2 Predicted Airflow and Hydrogen Concentration at Low Flow Rates

There is a need to understand fully, the effect of mechanical ventilation on hydrogen release and dispersion at the low airflow setting designed for the test room, which represents the highest risk situation. To simulate this situation, an air velocity of 0.567m/s was prescribed at each air exit vent. This corresponds with the minimum airflow rate of 0.317m^3/s at each vent, equivalent to 25% of the maximum capacity of the two air extraction fans. This airflow rate corresponds to 40 air changes per hour (ACH) for the laboratory under investigation. It is worthy of note that a ventilation rate of 30 ACH is required by the IGF code of Emergency Shut Down (ESD) designated space [5].

At the low airflow rates, CFD simulation calculated an average velocity of 2.5 m/s at the inlet region. As shown in Figure 4 (a), a near-uniform air exit velocity distribution was predicted along the direction of the airflow, with some localized regions of low-velocity field at the lower and upper area of the Test Cell, near the wall. This indicates that at the low exit velocity, the airflow pattern in the Test Cell may not be everywhere turbulent. The predicted velocity magnitude revealed the main air current is concentrated diagonally in the central part of the Test Cell, from the inlet to the exit vents. On either side of the main current, there is a weak velocity vortex, indicating lower turbulent intensity.

Figures 4 (c) and (d) show predicted hydrogen mass fraction from the steady-state simulation. Changes in hydrogen concentration are shown in representative contours of 14 colours, with a blue background representing minimum concentration, while the red colour represents regions within and above the LFL of hydrogen, of 0.3% by mass. The predicted hydrogen mass fraction from the steady-state simulation does not resolve the buoyant characteristics of the gas. This result is understandable because, the initial turbulent mixing with hydrogen in the ventilation airflow, is largely a time-dependent phenomenon. Consequently, additional simulations were conducted using time-dependent solution approach.

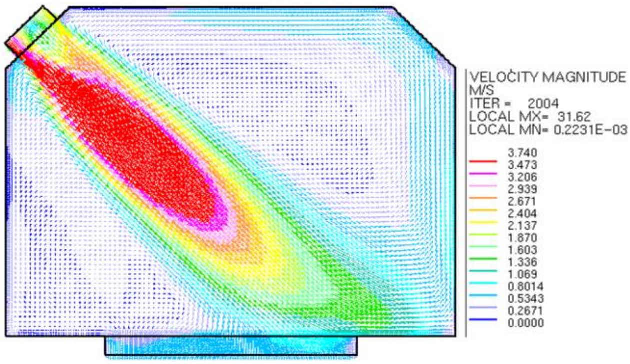

4(a) Refined grid: K-ε , UDS

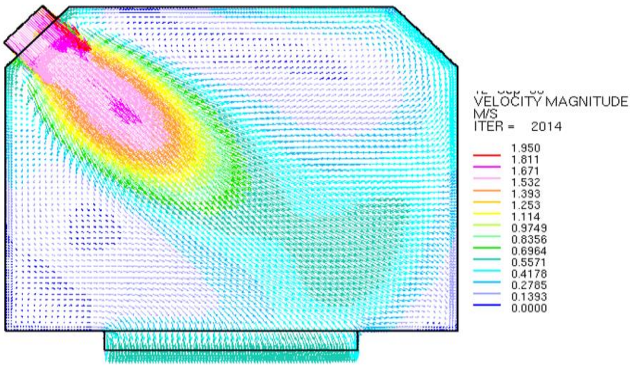

4(b) Non-refined grid: K-ε , UDS

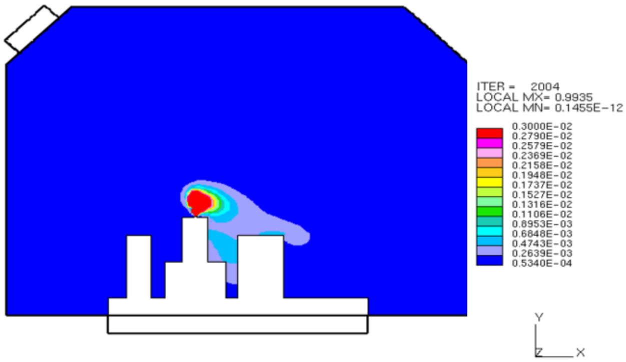

4(c) Refined grid. K-ε , UDS

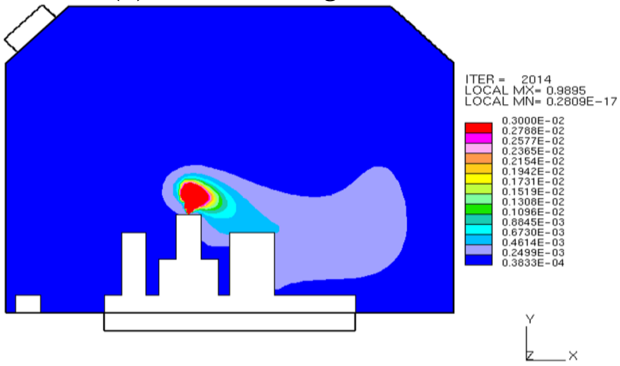

4(d) Non-refined grid: K-ε , UDS

Figure 4: Contour plots showing results from refined and non-refined grids, both at low airflow

4.3 Time-Dependent Analysis

Time-dependent or transient analysis involves approaching the steady-state solution through time steps. The $k - \varepsilon$ turbulence model with the MARS differencing scheme was used for this analysis at a time step of 0.01s for 10s. All other settings were as explained in previous sections. The first analysis was based on constant hydrogen leak from the same leak area and velocity. In the second case; the leak velocity was varied from 20.86 to 2m/s at a constant airflow of 0.567m/s, thus simulating the gradual shutdown of the hydrogen leak after detection.

4.4 Predicted Distribution of Hydrogen Gas with Constant Leak Rate

The solution obtained from the leakage of hydrogen at a constant leak rate of 20.86m/s using time-dependent analysis is shown in Figure 5. The Figure shows different levels of hydrogen plume concentration in the test room at time t = 2s, 3s, 6s and 7s. Results from the time-dependent solution resolve the buoyant characteristic of hydrogen gas rising upward towards the ceiling at time step 6s, which confirms the time-dependent nature of the problem. When compared with solutions obtained from the steady state approach, results from time-dependent analysis revealed a slightly lower level of hydrogen concentration, with a maximum value of 0.975. This suggests that the steady-state solution tends to over-predict the hydrogen concentration.

Analysis of results presented in Figure 5(a) revealed, the hydrogen gas initially rises to a height 0.55cm above the exit towards the ceiling, from where it gradually diffuses in a radial pattern to a homogenous non-flammable concentration in the room. This predicted pattern of hydrogen gas dispersion corresponds with the experimental and CFD results of Venetsanos et al. [16]. The study reported a fast transition to homogenous, non-flammable hydrogen distribution in the room. The shape of the region with a flammable concentration of hydrogen mass fraction shown in Figure 5(b) is similar in appearance to that predicted by the study of Kuldeep et al., [12], which simulates hydrogen leak of 3.0 x 10^{-5} kg/s with an airflow rate of 30 ACH in a room 7.3 m x 5.0m x 2.9m

($101m^3$). Despite the difference in ACH and size of the room between the two studies, the height of 37cm of flammable hydrogen region predicted by the study of Kuldeep et al. [12] agrees closely with the prediction in this study, which is 55cm.

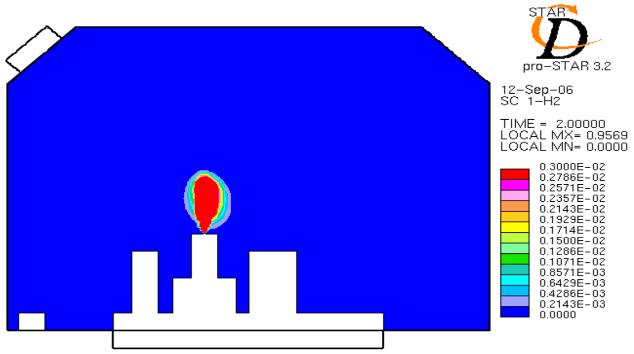

5(a) T = 2s

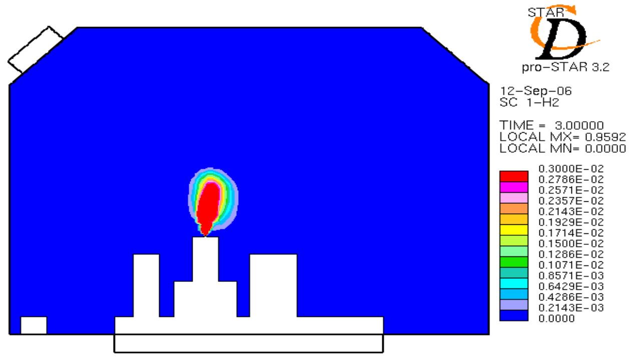

5(b) T = 3s

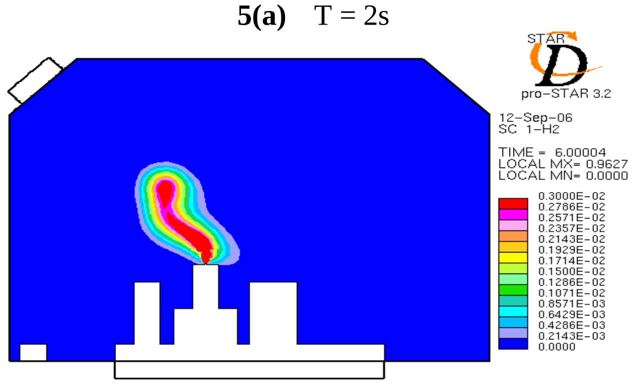

5(c) T = 6s

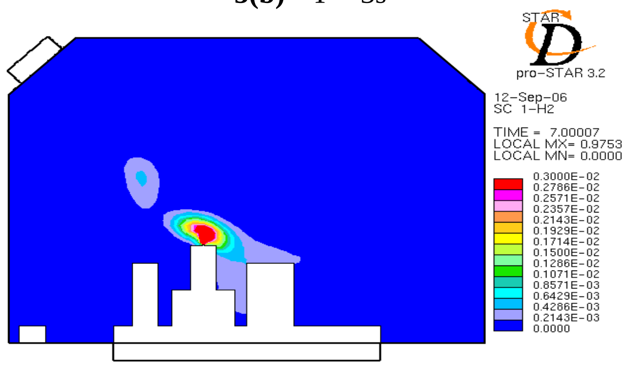

5(d) T = 7s

Figure 5: Concentration of hydrogen gas at various time steps

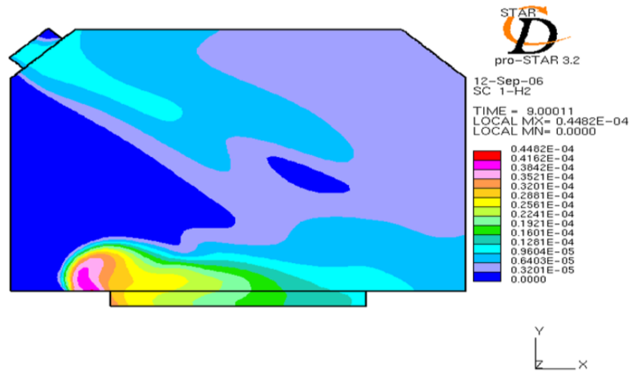

6(a) z = 0.713

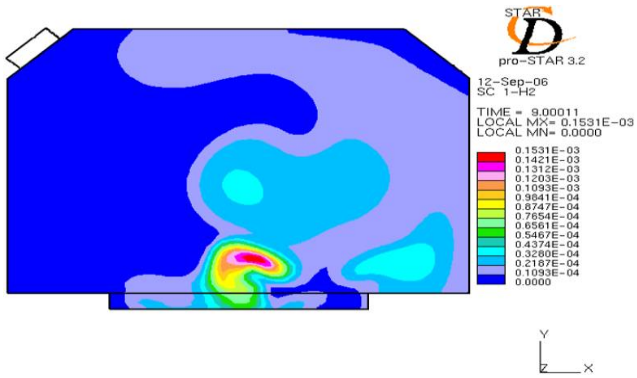

6(b) z = 0.297

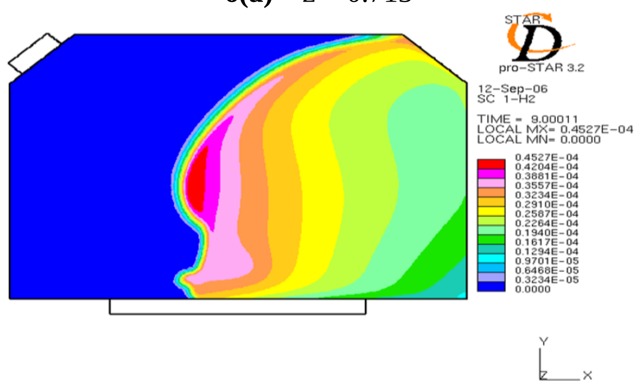

6(c) y = 0.995

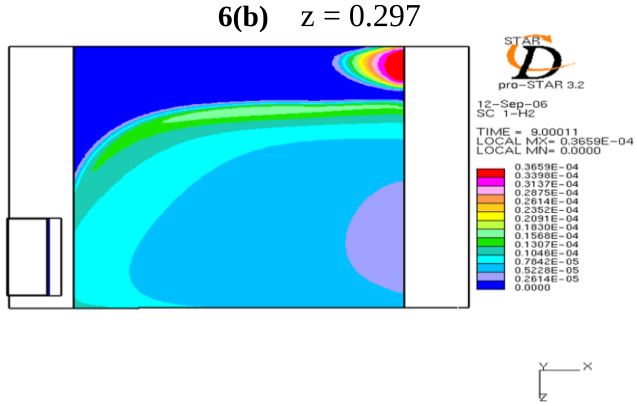

6(d) z = 0.005

Figure 6: Distribution of hydrogen gas at various parts of the Test Cell for transient simulation at T = 9s

Hydrogen gas normally rises and accumulates around the ceiling, when assisted by airflow in the same direction. However, in the Test Cell condition simulated in this study, the opposite direction of the ventilation airflow at 45^o to the horizontal produces a significant reduction in the buoyancy of hydrogen gas. This result agrees with the findings of Blaylock and Klebanoff [1], [5], which found that despite the inherent buoyancy of hydrogen, strong enough wind blows the gas downward. Furthermore, the lower Froud number of hydrogens released in this case study under strong opposing ventilation air is likely to have contributed to reducing the buoyancy effect of the released gas. This observation is consistent with that from a study by Brzezinska [2], [3], which found, that the lower the Froud Number, the lower the buoyancy force influences hydrogen dispersion.

In Figure 6, the predicted distribution of hydrogen gas close to the ceiling, floor, air inlet and exit vents as well as walls of the test room are presented. Higher concentration of the gas congregates on the walls and close to the air exit, revealing the influence of ventilation airflow on hydrogen dispersal. For the same reason, a smaller mass fraction of the gas was predicted in regions close to the ceilings and the air inlet. The contours around the air inlet also predict a small quantity of the gas being entrained in the air jet entering the room while a significant portion was convected through the air exit vents, with the main flow.

Generally, results from this study revealed, based on predicted hydrogen concentration in the Test Cell at the low airflow setting, any leakage of hydrogen gas would be dispersed from the Test Cell with the main airflow. This further proved that for the hydrogen leak considered in this study, even low airflow rates of 40ACH do not constitute a risk of fire in most parts of the room.

4.5 Time-Varying Leak Rate

The simulation of time-varying hydrogen concentration in the test room was done by changing the velocity of the leak source from 20.84 m/s to 2 m/s as plotted on the graph in Figure 7(a). The analysis was initialised based on the solution from the previous transient run, simulating the detection of the leak 10 seconds after initiation. Figure 7(b) shows changes in hydrogen concentration at different time steps for both transient cases 1 and 2. Prediction based on this simulation shows a decrease in hydrogen concentration with time, up to time 5s. Subsequently, a very low and constant maximum concentration of 0.001% was predicted.

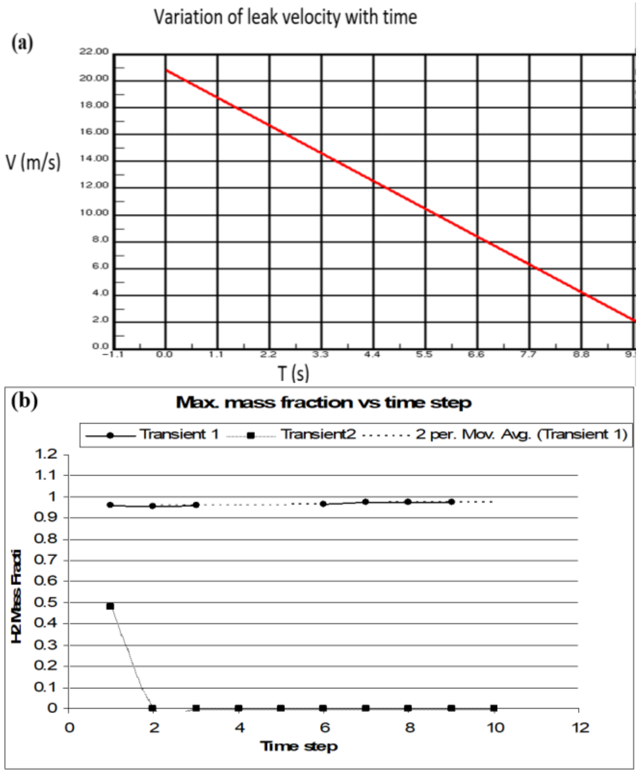

Figure 7: Changes in hydrogen concentration with time step for variable and constant hydrogen leak rate

4.6 Predicted Hydrogen Mass Fraction

The predicted hydrogen mass fraction presented in Figures 4 and 5 show that the highest concentration of hydrogen is restricted to the region of the leak source, which is near the geometric centre of the room. Away from this region, in other parts of the Test Cell, the predicted mass fraction of hydrogen at the low airflow settings was much below the LFL of the gas. This result agrees with the experimental and CFD results of Venetsanos et al. [16], which reported a fast transition to homogenous, non-flammable hydrogen distribution in the room. A similar result was obtained by Brzezinska [2], [3] and Malakhov et al. [17]. The latter study simulated small-size hydrogen release through an orifice of 0.8mm. The study reported that hydrogen concentration in the flammable region decreases as the distance from the leak point increases. Thus, the study concluded that the flammable region, near the leak source, is a dangerous location.

4.7 Effect of Discretization Schemes

In terms of predicted airflow pattern and hydrogen distribution, the UDS which is a first-order scheme predicted results that are consistent with the second-order schemes, such as MARS and LUD. The possible reason for this could be associated with the high density of the structured mesh of the Model used for the CFD analyses. This could have resulted in a damping effect on the numerical diffusion usually associated with the UDS. It is observed, that there is consistency in the predicted results of maximum and average hydrogen concentration in most parts of the Test Cell as calculated by most of the schemes and turbulence models, except for a small difference in the calculated minimum value.

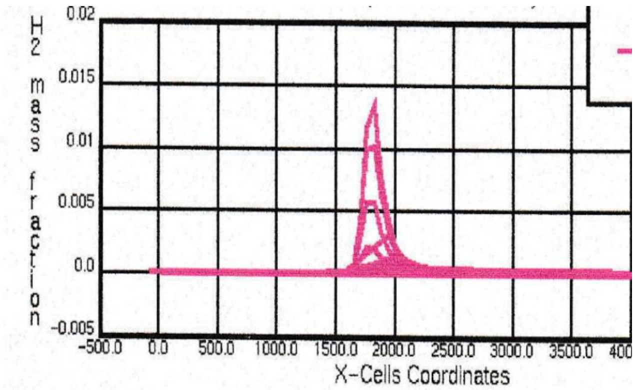

Figure 8: Predicted axial profile of hydrogen mass fraction at z = 0.5 (Centre of Test Cell)

Most of the schemes predicted a maximum concentration of hydrogen in the test room in the region of 1.4%, which is restricted to the cells close to the leak source as shown in the graph in Figure 8. Hence, it can be concluded that for the type of leak considered in this study and at the low airflow setting, hydrogen leak does not constitute risk of fire in most parts of the test room, except in the region close to the leak source.

5.0 CONCLUSIONS

Airflow and hydrogen leak in a HCCI engine laboratory modified to operate with hydrogen fuel were numerically simulated using steady-state and time-dependant solution approaches. The calculations were based on RANS-based turbulence models and differencing schemes. The predicted velocity magnitude revealed the main air current is concentrated in the central part of the Test Cell, from the inlet to the exit vents. On either side of the main airflow, there is a weak velocity vortex, indicating lower turbulent intensity. The predicted hydrogen mass fraction from the steady-state simulation does not resolve the buoyant characteristics of the gas. In contrast, results from the time-dependent solution resolve the buoyant of the hydrogen plume. It revealed, that the hydrogen gas initially rises to a height 0.55cm above the exit towards the ceiling, from where it gradually diffuses in a radial pattern to a homogenous non-flammable concentration in the room. This predicted pattern of hydrogen gas dispersion is consistent with experimental and CFD data reported previously. The study indicates the region of the test room with hydrogen concentration above the lower flammability limit was restricted to the small area of the leak source. Additionally, the predicted distribution of hydrogen gas in a significant portion of the Test Cell was below 25% of the lower flammability limit of hydrogen (4% volume or 0.3% mass), even at the lower airflow settings. Consequently, it was inferred that the release of hydrogen gas from a small leak area of the type investigated in this study; at low ventilation airflow designed for the test room does not constitute a risk of fire.

REFERENCES

[1] Blaylock, M. L., and Klebanoff, L. E., "Hydrogen gas dispersion studies for hydrogen fuel cell vessels I: Vent Mast releases", International Journal of Hydrogen Energy, Volume 47, Issue 50,2022,Pages 21506-21516,ISSN 0360-3199, https://doi.org/10.1016/j.ijhydene.2022.04.26.

[2] Brzezińska, D. "Hydrogen dispersion and ventilation effects in enclosures under different release conditions", *Energies*, 2021, 14(13). https://doi.org/10.3390/en14134029

[3] Brzezińska, D. "Hydrogen dispersion phenomenon in nominally closed spaces", *International Journal of Hydrogen Energy*, 2021, 46(55), 28358–28365. https://doi.org/10.1016/j.ijhydene.2021.06.061

[4] Compressed Gas Association, *Handbook of compressed gases Springer New York*, 1999, 4th edn., ISBN 978-0-412-78230-5,703 pp.

[5] Gitushi, K. M., Blaylock, M. L., and Klebanoff, L. E. "Hydrogen Gas Dispersion Studies for Hydrogen Fuel Cell Vessels II: Fuel Cell Room Releases and the Influence of Ventilation Introduction", 2022.

[6] Tanaka, T., Azuma, T., Evans, J. A., Cronin, P. M., Johnson, D. M., and Cleaver, R. P. "Experimental study on hydrogen explosions in a full-scale hydrogen filling station model", *International Journal of Hydrogen Energy*, 2007, 32(13), 2162–2170. https://doi.org/10.1016/j.ijhydene.2007.04.019

[7] Wang, T., Yang, F., Hu, Q., Hu, S., Li, Y., and Ouyang, M. "Experimental and simulation research on hydrogen leakage of double ferrule joints", *Process Safety and Environmental Protection*, 2022, 160, 839–846.

[8] Machniewski, Piotr, and Eugeniusz Molga "CFD Analysis of Large-Scale Hydrogen Detonation and Blast Wave Overpressure in Partially Confined Spaces", *Process Safety and Environmental Protection*, 2022, 158: 537–46.

https://www.sciencedirect.com/science/article/pii/S0957582021007060.

[9] Choi, J., Hur, N., Kang, S., Lee, E. D., and Lee, K. B. “A CFD simulation of hydrogen dispersion for the hydrogen leakage from a fuel cell vehicle in an underground parking garage”, *International Journal of Hydrogen Energy*, 2013, vol. 38, no. 19, pp. 8084–8091, doi:10.1016/j.ijhydene.2013.02.018.

[10] Tolias, I. C., Stewart, J. R., Newton, A., Keenan, J., Makarov, D., Hoyes, J. R., Molkov, V., and Venetsanos, A. G. “Numerical simulations of vented hydrogen deflagration in a medium-scale enclosure”, *Journal of Loss Prevention in the Process Industries*, 2018, Volume 52, Pages 125-139, ISSN 0950-4230, https://doi.org/10.1016/j.jlp.2017.10.014.

[11] Zhao, M., Huang, T., Liu, C., Chen, M., Ji, S., Christopher, D. M., and Li, X. “Leak localization using distributed sensors and machine learning for hydrogen releases from a fuel cell vehicle in a parking garage”, *International Journal of Hydrogen Energy*, 2021, Volume 46, Issue 1, Pages 1420-1433, ISSN 0360-3199, https://doi.org/10.1016/j.ijhydene.2020.09.218.

[12] Prasad, K., Pitts, W., and Yang, J. “Effect of wind and buoyancy on hydrogen release and dispersion in a compartment with vents at multiple levels”, *International Journal of Hydrogen Energy*, 2010, Volume 35, Issue 17, Pages 9218-9231, ISSN 0360-3199, https://doi.org/10.1016/j.ijhydene.2010.06.001.

[13] Lawal, M. S., Fairweather, M., Gogolek, P., Ingham, D. B., Ma, L., Pourkashanian, M., and Williams, A. “CFD predictions of wake-stabilised jet flames in a cross-flow”, *Energy*, 2013, 53, 259–269. https://doi.org/10.1016/j.energy.2013.02.020

[14] Seike, M., Kawabata, N., Hasegawa, M., and Tanaka, H. “Heat release rate and thermal fume behavior estimation of fuel cell vehicles in tunnel fires”, *International Journal of Hydrogen Energy*, 2019, 44(48), 26597–26608.

[15] LaNasa, P. J., and Loy, E. “Upp, 2 - Basic Flow Measurement Laws”, Fluid Flow Measurement (Third Edition), *Butterworth-Heinemann*, 2014, Pages 19-29, ISBN 9780124095243, https://doi.org/10.1016/B978-0-12-409524-3.00002-2.

[16] Venetsanos, A. G., Papanikolaou, E., Delichatsios, M., Garcia, J., Hansen, O. R., Heitsch, M., Huser, A., Jahn, W., Jordan, T. , Lacome, J. M., Ledin, H. S., Makarov, D., Middha, P., Studer, E., Tchouvelev, A. V., Teodorczyk, A., Verbecke, F., and Van der Voort, M. M., “An inter-comparison exercise on the capabilities of CFD models to predict the short and long term distribution and mixing of hydrogen in a garage”, *International Journal of Hydrogen Energy*,Volume 34, Issue 14, 2009, Pages 5912-5923, ISSN 0360-3199, https://doi.org/10.1016/j.ijhydene.2009.01.05.

[17] Malakhov, A. A., Avdeenkov, A. V., du Toit, M. H., and Bessarabov, D. G. “CFD Simulation and Experimental Study of a Hydrogen Leak in a Semi-Closed Space with the Purpose of Risk Mitigation.” *International Journal of Hydrogen Energy*, 2020, 45(15): 9231–40. https://www.sciencedirect.com/science/article/pii/S0360319920300999.